Apatite formation on a hydrogel containing sulfinic acid group under physiological conditions

Ryo Hamai[1], Yuki Shirosaki[2], Toshiki Miyazaki[1,*]

[1]Graduate School of Life Science and Systems Engineering, Kyushu Institute of Technology, Japan

[2]Frontier Research Academy for Young Researchers, Kyushu Institute of Technology, Japan

*** Corresponding author:**

Toshiki Miyazaki

Graduate School of Life Science and Systems Engineering, Kyushu Institute of Technology, 2-4, Hibikino, Wakamatsu-ku, Kitakyushu 808-0196, Japan.

Tel/Fax: +81-93-695-6025

E-mail: tmiya@life.kyutech.ac.jp

Abstract

Natural bone consists of apatite and collagen fiber. Bioactive materials capable to bonding to bone tissue are clinically used as bone-repairing materials. Apatite-organic polymer composites exhibit bone-bonding abilities and mechanical properties similar to those of natural bone, and these materials can be prepared using biomimetic processes in simulated body fluid (SBF). Specific functional groups such as sulfonic and carboxylic acid groups are known to induce the heterogeneous nucleation of apatite in SBF. However, it remains unclear whether structurally related sulfinic acid groups can contribute to apatite formation in the same way, despite sodium sulfonate being used in biomedical applications as a radical polymerization promoter in adhesive dental resin. Herein, we report the preparation of a new hydrogel containing sulfinic acid groups from sodium 4-vinylbenzenesulfinate and 2-hydroxyethyl methacrylate using a radical polymerization reaction and the subsequent incorporation of Ca^{2+} ions into this material. We also investigated the apatite forming behavior of these hydrogels in SBF. Hydrogels containing sulfinic acid groups showed higher apatite-forming ability than those without sulfinic acid groups. In addition, the apatite layer formed on the former showed tight adhesion to the hydrogel. This phenomenon was attributed to the heterogeneous nucleation of apatite, induced by the sulfinic acid groups.

Running heads: Apatite formation on a hydrogel containing sulfinic acid group

1. Introduction

Bone-bonding bioactivity is one of the most important properties of any prospective bone-repairing material. This property can be achieved between artificial materials and bone tissues under physiological condition through the formation of a low-crystalline apatite layer. Bioglass [1], glass-ceramics A-W [2] and sintered hydroxyapatite [3] have all been used in clinical practice as bone substitutes because they exhibit both bioactivity and high mechanical strength. The regeneration of bone tissue can be enhanced by varying the loading of the bone-repairing material. However, implanted ceramics may inhibit the transmission of load to the surrounding bone (i.e., stress shielding), which can lead to bone absorption.

To address this issue, considerable research efforts have been directed towards the fabrication of novel bioactive organic-inorganic composites showing mechanical properties similar to those of natural bone. Biomimetic processes using simulated body fluid (SBF) have been evaluated in detail to develop new methods for the preparation of apatite-organic polymer composites [4]. SBF is solution supersaturated with respect to apatite and its composition of inorganic ion nearly equals to human blood plasma [5]. The functional groups responsible for inducing heterogeneous nucleation in SBF govern the formation of apatite on the surface of a given substrate. Several functional groups have been reported to induce nucleation, including carboxylic acid (-COOH) [6], sulfonic acid ($-SO_3H$) [7] and phosphonic acid ($-PO_3H_2$) [6] groups. Moreover, the release of any

chemical species leading to an increase in the degree of supersaturation with respect to apatite in SBF can promote apatite formation [8]. The incorporation of functional groups with apatite-forming abilities into organic polymers, as well as the addition of chemical species capable of increasing the degree of supersaturation, are therefore important for obtaining composites using this process.

Sulfinic acid groups ($-SO_2H$) are S-containing groups that have a similar chemical structure to sulfonic acid groups. Sodium *p*-toluenesulfinate (*p*-TSS) and sodium benzenesulfinate are used commercially to accelerate the radical polymerization reaction of the acidic monomers used in dental resin [9-10]. We previously examined the effects of *p*-TSS on the formation of apatite from vinylphosphonic acid-based copolymers in SBF [11]. The results of our previous study showed that *p*-TSS led to an improvement in the chemical durability of the copolymer under aqueous conditions.

Although the induction of apatite formation by sulfonic acid groups in SBF has been reported previously by several other research groups, the effects of sulfinic acid groups on apatite formation remain unclear. Difference in chemical structure of functional groups containing the same element is expected to affect the strength of interaction with ion in SBF, thereby leading to different behavior of apatite formation. Furthermore, it is expected that a thorough comparison of sulfinic and sulfonic acid groups in this context will provide fundamental insights into the relationship between chemical structure of functional group and

biomineralization behavior. If organic polymer containing this kind of functional group induces apatite formation, it is expected to be useful for the injectable hydrogel for bone repair.

In this study, we have prepared model hydrogels containing sulfinic acid groups and calcium ions by the radical polymerization of sodium 4-vinylbenzenesulfinate ($VBSO_2$) and 2-hydroxyethyl methacrylate (HEMA). The apatite forming behaviors of the resulting poly $VBSO_2$-HEMA hydrogels with various sulfinic acid group contents were investigated to clarify the potential apatite-forming abilities of sulfinic acid groups in SBF.

2. Material and methods

2.1. Preparation of the different hydrogels

$VBSO_2$ and HEMA were used as monomer to prepare the hydrogel. *N*,*N*'-methylenebisacrylamide is the cross-linking agent for the hydrogel. Moreover *N*,*N*,*N*',*N*'-tetramethylethylenediamine and 2,2'-azobis(2-methylpropionamidine) dihydrochloride are initiator for radical polymerization. $VBSO_2$ (90%, Tokyo Chemical Industry Co., Ltd, Tokyo, Japan) and HEMA (95%, Wako Pure Chemical Industries, Ltd, Osaka, Japan) were used as monomers with a total charge of 0.01 mol. Two different reactions were conducted with $VBSO_2$ ratios of 0 and 10 mol% relative to the total amount of monomer. The materials resulting from these reactions will be referred to

hereafter as $0VBSO_2$ and $10VBSO_2$, respectively. *N*,*N*'-methylenebisacrylamide (99%, Wako Pure Chemical Industries) and *N*,*N*,*N*',*N*'-tetramethylethylenediamine (98%, Wako Pure Chemical Industries) were added at 1 and 0.15 mol%, respectively, to the total monomers, and the resulting mixtures were dissolved in ultra-pure water passed through reverse osmosis membrane, ion-exchange resin column, and membrane filter using a purification system (Direct-Q, Millipore, Germany). The aqueous solutions were then stirred for 5 min and adjusted to a total volume of 10 mL in a volumetric flask. 2,2'-azobis(2-methylpropionamidine) dihydrochloride (95%, Wako Pure Chemical Industries; 1 mol% relative to the total amount of monomer) was then added to the solution, and a small sampled (1 mL) of the resulting mixture was poured into the polypropylene cup and polymerized at 60 °C for 1 day.

The hydrogels prepared in this way were dried at room temperature for 1 day, before being cut into squares of 10 × 10 mm in size. The hydrogels were then soaked in 30 mL of a 0.01 or 0.05 M calcium chloride ($CaCl_2$) solution at 36.5 °C for 1 day. The hydrogels were then washed in ultrapure water and dried at room temperature for 1 day.

2.2. Soaking of specimen in SBF and Tris-NaCl buffer

SBF (Na^+ 142.0, K^+ 5.0, Mg^{2+} 1.5, Ca^{2+} 2.5, Cl^- 147.8, HCO_3^- 4.2, HPO_4^{2-} 1.0, SO_4^{2-} 0.5 mM) was prepared by the sequential addition of NaCl, $NaHCO_3$, KCl, $K_2HPO_4 \cdot 3H_2O$, $MgCl_2 \cdot 6H_2O$, $CaCl_2$ and Na_2SO_4 (Nacalai

Tesque, Inc., Kyoto, Japan) to ultra-pure water. The pH of the resulting solution was adjusted to 7.4 by the addition of tris(hydroxymethyl) aminomethane (Nacalai Tesque, Inc.) and the appropriate volume of a 1.0 M hydrogen chloride (HCl) solution. The hydrogels were then soaked in 30 mL of SBF at 36.5 °C for 5 days.

Tiris-NaCl buffer was used for measurement of calcium ion release form hydrogel under simple condition in comparison with SBF. Tris-NaCl buffer (NaCl 142, tris(hydroxymethyl) aminomethane 50 mM) was prepared by dissolving NaCl and tris(hydroxymethyl) aminomethane in ultra-pure water. The pH of the resulting solution was adjusted to 7.40 using 1.0 M HCl solution. The hydrogels were soaked in 30 mL of Tris-NaCl buffer at 36.5 °C for 12 h.

2.3. Characterization

The chemical structures of the hydrogels were analyzed before being soaked in $CaCl_2$ solution by Fourier transform infrared spectroscopy (FT-IR; FT/IR-6100, JASCO Co., Tokyo, Japan) using an attenuated total reflectance method. The scan range for the FT-IR analysis was set from 950 to 2000 cm^{-1} at a resolution of 4 cm^{-1}. The Ca contents of the hydrogels were determined after being soaked in $CaCl_2$ solution by energy dispersive X-ray (EDX) analysis using an EMAX Energy system (Horiba Ltd, Kyoto, Japan) equipped with a scanning electron microscope (SEM; S-3500N; Hitachi Co., Tokyo, Japan). The surfaces of the hydrogels were coated with carbon using a carbon coater (CADE,

Meiwafosis Co., Ltd, Osaka, Japan) immediately prior to the Ca content measurements.

After being soaked in SBF for various time periods, structural changes in the surfaces of the hydrogels were characterized by thin-film X-ray diffraction (TF-XRD; MXP3V, Mac Science, Co., Yokohama, Japan) and SEM. Monochromated Cu-Kα radiation was used for the TF-XRD analysis, which was fixed at 1° against the surface of each hydrogel specimen with a scan rate of 0.02° sec^{-1}. Furthermore, the adhesion strength of the apatite formed on the specimen was evaluated using a peel-off test. Chukoh Flo® adhesive tape (ASF-110 FR, Chukoh Chemical Industries, Ltd, Tokyo, Japan) was attached to the surface of each hydrogel specimen formed with the apatite and then peeled off. The surface of each specimen was then tested by SEM.

The concentrations of Ca and P in the Tris-NaCl buffer and SBF following the soaking of the hydrogel specimens were measured by inductively coupled plasma optical emission spectrometry (ICP-OES; Optima 4300DV CYCLON, Perkin-Elmer Inc., London, UK).

3. Results

Figure 1 shows the FT-IR spectra of the hydrogels prepared using different amounts of $VBSO_2$ before being soaked in $CaCl_2$ solution. In all cases, the stretching vibrations of the C=O, O–C (alcohol) and C–O (ester) bonds

derived from HEMA were observed at 1706, 1074 and 1023 cm^{-1}, respectively [11]. A peak was also observed at 1165 cm^{-1} for all of the hydrogel specimens prepared in the current study, which was attributed to the vibration and torsion of the CH_3 and OH groups of HEMA, respectively. Furthermore, peaks corresponding to amide I were also observed at 1635 cm^{-1} [12] for both hydrogel specimens. Peaks also appeared at 1030 and 1008 cm^{-1}, which were assigned to the in-plane deformation vibrations of the S=O [13] and C–H bonds, respectively, but these were only observed in the spectrum of $10VBSO_2$.

Figure 2 (A) shows the Ca contents of the different hydrogels after they were soaked in various concentrations of $CaCl_2$ solution. The Ca content of $10VBSO_2$ was found to be larger than that $0VBSO_2$ regardless of the $CaCl_2$ concentration. Figure 2 (B) shows the Ca concentration in Tris-NaCl buffer following the soaking of each hydrogel for 12 h. The amount of Ca released from $10VBSO_2$ following its soaking in Tris-NaCl buffer was higher than that of $0VBSO_2$ regardless of the $CaCl_2$ concentration.

Figure 3 shows TF-XRD patterns of the different hydrogel specimens after they had been soaked in SBF for various time periods. The $10VBSO_2$ hydrogel gave broad peaks at $2\theta = 26$ and 32° after being soaked for 12 h in a 0.01 M solution of $CaCl_2$, which were attributed to the formation of apatite. However, the $0VBSO_2$ hydrogel did not show any peaks corresponding to apatite, even after 5 days under the same conditions. Apatite peaks were observed for both materials after 12 h for the hydrogels treated with a 0.05 M $CaCl_2$ solution.

Figure 4 shows SEM images of the different hydrogels after being soaked in SBF for 5 days. The SEM image of the $0VBSO_2$ hydrogel treated with a 0.05 M solution of $CaCl_2$ revealed that the material adopted a spherical morphology following the deposition of apatite, with a gap forming between the surface and the deposited material. The SEM images of the $10VBSO_2$ hydrogel treated with 0.01 and 0.05 M solutions of $CaCl_2$ revealed the formation of a continuous layer of deposited material, which sat in close contact with the surface.

Figure 5 show the SEM images of the $0VBSO_2$ and $10VBSO_2$ hydrogels treated with a 0.05 M solution of $CaCl_2$, before being soaked in SBF for 1 day and subjected to a peeling-off test using tape. Almost all of the deposited material formed on the surface of the $0VBSO_2$ hydrogel was removed after the test, whereas the deposited material on the $10VBSO_2$ hydrogel remained intact.

Figure 6 shows the P concentrations of the SBF after it was used to soak the different hydrogels for various times periods. The results revealed that the P concentration remained almost constant for the $0VBSO_2$ hydrogel treated with a 0.01 M $CaCl_2$ solution regardless of the soaking time. The reduction in the P concentration was of the order $0VBSO_2$ treated with 0.05 M $CaCl_2$ < $10VBSO_2$ treated with 0.05 M $CaCl_2$ < $10VBSO_2$ treated with 0.01 M $CaCl_2$.

4. Discussion

FT-IR analysis revealed that the hydrogel prepared from $VBSO_2$ and HEMA contained S=O and C–OH bonds from the two different monomers, respectively (see Figure 1). This result therefore confirmed that the sulfinic acid groups had been successfully incorporated into the hydrogel by the radical polymerization reaction.

All of the hydrogels prepared in the current study containing sulfinic acid groups formed apatite regardless of the $CaCl_2$ concentration, whereas those without sulfinic acid groups formed apatite only after being treated with 0.05 M $CaCl_2$ (see Figure 3). The level of P consumption observed after the soaking of the $10VBSO_2$ hydrogel pretreated with 0.05 M $CaCl_2$ in SBF was higher than that observed for the $0VBSO_2$ material under the same conditions (see Figure 6). This result therefore means that a much larger amount of apatite was formed on the surface of the $10VBSO_2$ hydrogel compared with the $0VBSO_2$ material. Taken together, these results revealed that the incorporation of sulfinic acid groups enhanced the apatite-forming ability of the hydrogel.

More Ca^{2+} ions were released into the Tris-HCl buffer from the $10VBSO_2$ hydrogel pretreated with $CaCl_2$ than the corresponding $0VBSO_2$ material, irrespective of the $CaCl_2$ concentration (See Figure 2(A) and (B)). This result therefore indicated that the incorporated sulfinic acid groups were playing a critical role in the binding of the Ca^{2+} ions. Furthermore, it has been reported that Ca^{2+} adsorption increases as the swelling ratio of a hydrogel increases in $CaCl_2$ solution [14]. Electrostatic repulsion between ionic functional groups is one of

the major influencing factors involved in swelling of hydrogels [15]. The presence of sulfinic acid groups on the hydrogel would therefore make a considerable contribution to the incorporation and subsequent release of Ca^{2+} to accelerate apatite formation.

The sulfinic acid groups on the hydrogel also affected the morphological characteristics of the deposited apatite (see Figure 4). This change in the morphology was attributed to differences in the apatite nucleation process. The apatite formed on the $10VBSO_2$ hydrogel adopted a continuous layered structure, which shared similar morphological characteristics to apatite formed on titanium metal treated with NaOH [16] and polyamide film containing carboxylic acid groups [17]. The sulfinic acid groups on the surface of the hydrogel would be almost completely ionized and negatively charged in SBF, given that the acid dissociation constant (pKa) of benzenesulfinic acid is 1.29 [18]. Also, it is well known that ion–ion interactions between negatively charged functional groups and Ca^{2+} ions can contribute to the heterogeneous nucleation of apatite in SBF [6]. Taken together, these results indicate that the apatite layer on the $10VBSO_2$ hydrogel was formed by heterogeneous nucleation.

In contrast, the $0VBSO_2$ hydrogel treated with 0.05 M $CaCl_2$ formed an assembly of particulate apatite in SBF. For homogeneous nucleation, particulate apatite tends to be precipitated by an increase in the degree of supersaturation in SBF [19]. The main hydrophilic groups on the surface of this hydrogel would be the hydroxyl groups derived from HEMA, which would lead to the formation of

ion–polar interactions with the Ca^{2+} ions [6]. However, these interactions are much less likely to result in heterogeneous apatite nucleation than ion–ion interactions, and it was therefore assumed that homogeneous nucleation was preferentially induced by the release of Ca^{2+} ions to grow into spherical particles.

Moreover, the apatite adhered to the surface of the $10VBSO_2$ hydrogel much more strongly than it did to the $0VBSO_2$ material (see Figure 5). The interactions formed between the anionic functional groups and the Ca^{2+} ions therefore not only affected the heterogeneous nucleation but also resulted in the tight adhesion of the apatite layer, in a similar manner to polyamide films containing carboxylic acid groups [17].

It has been reported that polyethylene substrates modified with sulfonic acid groups formed apatite within 3 days in SBF when they were treated with saturated aqueous $Ca(OH)_2$ solution [20]. In contrast, the present hydrogel formed apatite after only 12 h in SBF. Although it is difficult to make a direct comparison between these systems because of the differences in the sample preparation and Ca-incorporation conditions, it is assumed that sulfinic acid group is one of the functional groups that induce the apatite formation. The preparation and subsequent evaluation of the apatite forming abilities of hybrids containing sulfonic or sulfinic acid groups using the same methods would therefore be required to determine the overall impact of this structural change.

Taken together, the results of this study have revealed that sulfinic acid groups may be used to induce the heterogeneous nucleation of apatite in SBF. It

is therefore envisaged that the incorporation of this group into a polymer matrix could be used as a general strategy for the fabrication of apatite-polymer composites using SBF. Moreover, based on the material design strategy presented in the current study, it is envisaged that polymer material containingng sulfinic acid groups could integrate with teeth as phosphate groups in the dental resin.

5. Conclusions

The apatite formation behavior of poly $VBSO_2$-HEMA hydrogels has been examined in SBF. The results revealed that the sulfinic acid groups on the surfaces of these hydrogels induced the heterogeneous nucleation of apatite under physiological conditions and contribute to the fabrication of apatite-organic polymer composites though biomimetic processes using SBF.

References

1 Hench LL. Bioceramics. J Am Ceram Soc 1998;81:1705–1728.

2 Kokubo T, Kim HM, Kawashita M. Novel bioactive materials with different mechanical properties. Biomaterials 2003;24:2161–2175.

3 Jarcho M, Bolen CH, Thomas MB, Bobick J, Kay JF, Doremus RH. Hydroxyapatite synthesis and characterization in dense polycrystalline forms. J Mater Sci 1976;11:2027–2035.

4 Ohtsuki C, Kamitakahara M, Miyazaki T. Coating bone-like apatite onto organic substrates using solutions mimicking body fluid. J Tissue Eng Regen Med 2007;1:33–38.

5 Kokubo T, Takadama H. How useful in SBF in predicting in vivo bone bioactivity? Biomaterials 2006;27:2907–2915.

6 Tanahashi M, Matsuda T. Surface functional group dependence on apatite formation on self-assembled monolayers in a simulated body fluid. J Biomed Mater Res 1997;34:305–315.

7 Kawai T, Ohtsuki C, Kamitakahara M, Miyazaki T, Tanihara M, Sakaguchi Y, Konagaya S. Coating of an appetite layer on polyamide films containing sulfonic groups by a biomimetic process. Biomaterials 2004;25:4529–4534.

8 Koh MY, Ohtsuki C, Miyazaki T. Modification of polyglutamic acid with silanol groups and calcium salts to induce calcification in a simulated body fluid. J Biomater Appl 2011;25:581–594.

9 Yamauchi J, Study of dental adhesive resin containing phosphoric acid methacrylate monomer. J Jpn Soc Dent Mater Devices 1986;5:144–154 (in Japanese).

10 Van Landuyt KL, Snauwaert J, De Munck J, Peumans M, Yoshida Y, Poitevin A, Coutinho E, Suzuki K, Lambrechts P, Van Meerbeek B. Systematic review of the chemical composition of contemporary dental adhesives. Biomaterials 2007;28:3757–3785.

11 Ferreira L, Vidal MM, Gil MH. Evaluation of poly(2-hydroxyethyl methacrylate) gels as drug delivery system at different pH value. Int J Pharm 2000;194:169–180.

12 Liu M, Liu H, Liu Y, Bai L, Yang G, Yang C, Cheng J, Preparation and characterization of temperature-responsive poly (*N*-isopropylacrylamide-co-*N*, *N*'-methylenebisacrylamaide) monolith for HPLC, J Chromatogr A 2011:1218:286-292.

13 Halm C, Evarts J, Kurth MJ. A new attachment / cleavage strategy: polymer-bound allylic sulfones in a solid-phase route to trisubstituted olefins. Tetrahedron Lett 1997;38:7709–7712.

14 Nakata R, Miyazaki T, Morita Y, Ishida E, Iwatsuki R, Ohtsuki C. Apatite formation abilities of various carrageenan gels in simulated body environment. J Ceram Soc Japan 2010;118:487–490.

15 Hassan CM, Doyle III FJ, Peppas NA. Dynamic behavior of glucose-responsive poly(methacrylic acid-γ-ethylene glycol) hydrogels. Macromolecules 1997;30:6166–6173.

16 Kim HM, Miyaji F, Kokubo T, Nakamura T. Preparation of bioactive Ti and its alloys via simple chemical surface treatment. J Biomed Mater Res 1996;32:409–419.

17 Miyazaki T, Ohtsuki C, Akioka Y, Tanihara M, Nakao J, Sakaguchi Y, Konagaya S. Apatite deposition on polyamide films containing carboxyl group in a biomimetic solution. J Mater Sci Mater Med 2003;14:569–574.

18 Veltwish D, Janata E, Asmus KD. Primary processes in the reaction if OH·-radicals with sulphoxides. J Chem Soc Perkin Trans 1980;2:146–153.

19 Yamaguchi S, Yabutsuka T, Hibino M, Yao T. Formation of apatite pattern by electrophoretic deposition of apatite nuclei. Key Eng Mater 2007;330-332:3–6.

20 Leonor IB, Kim HM, Balas F, Kawashita M, Reis RL, Kokubo T, Nakamura T. Surface potential change in bioactive polymer during the process of biomimetic apatite formation in a simulated body fluid. J Mater Chem 2007;17:4057–4063.

Figure captions

Figure 1 FT-IR spectra of the different hydrogel specimens before being soaked in $CaCl_2$ solution (▲: ν(C=O) of HEMA; ■: amide I; △: γ(CH_3) or τ(OH) of HEMA; ◆: ν(O–C) alcohol of HEMA; ●: S=O bond of $VBSO_2$; ◇: ν(C–O) ester of HEMA; ○: C–H bond n-plane deformation vibration of $VBSO_2$; ν is stretching; γ is rocking; τ is torsion.).

Figure 2 Ca contents of the different hydrogels after soaking in various concentrations of $CaCl_2$ solution (A) and the Ca concentrations of the hydrogels after soaking in Tris-NaCl buffer for 12 h (B) ($N = 3$).

Figure 3 TF-XRD patterns of the surfaces of the specimens after soaking in SBF for various periods.

Figure 4 SEM images of the different hydrogel specimens after being soaked in SBF for 5 d.

Figure 5 SEM images of the surfaces of the different hydrogel specimens treated with a 0.05 M solution of $CaCl_2$ before and after being soaked in SBF for 1 day, which were all subjected to the peeling-off test.

Figure 6 Change in the P concentrations of the different hydrogels after being soaked in SBF.

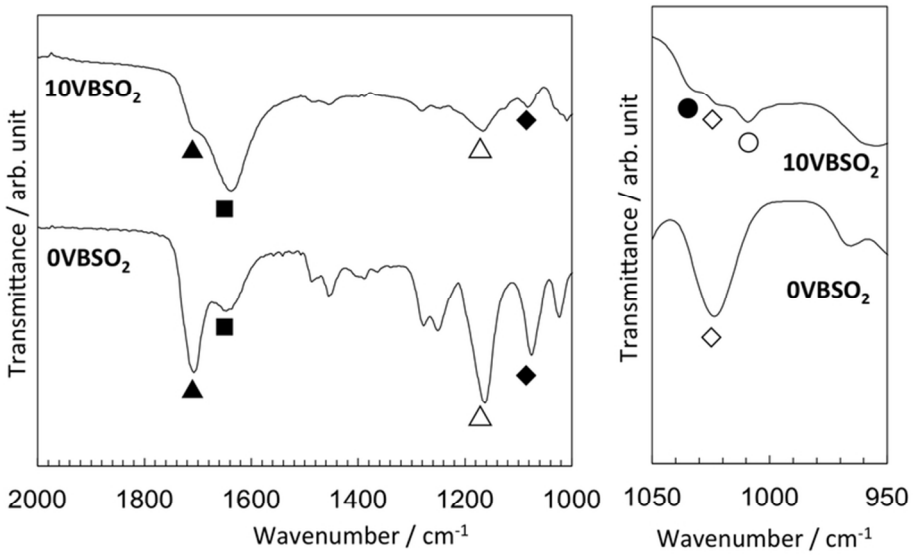

Figure 1

75x54mm (300 x 300 DPI)

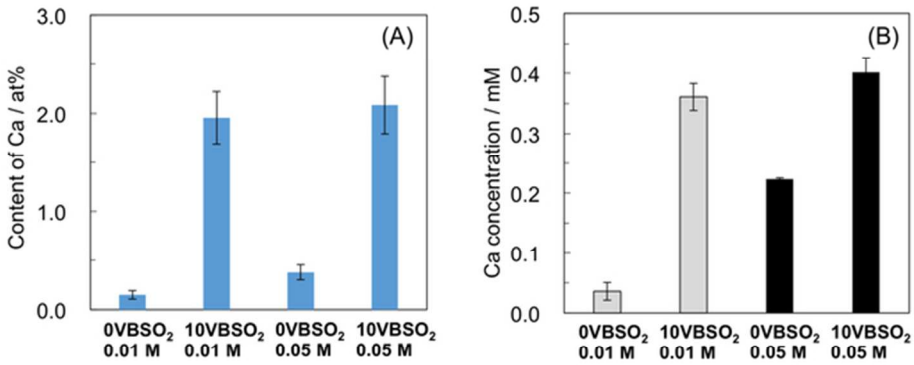

Figure 2

61x35mm (300 x 300 DPI)

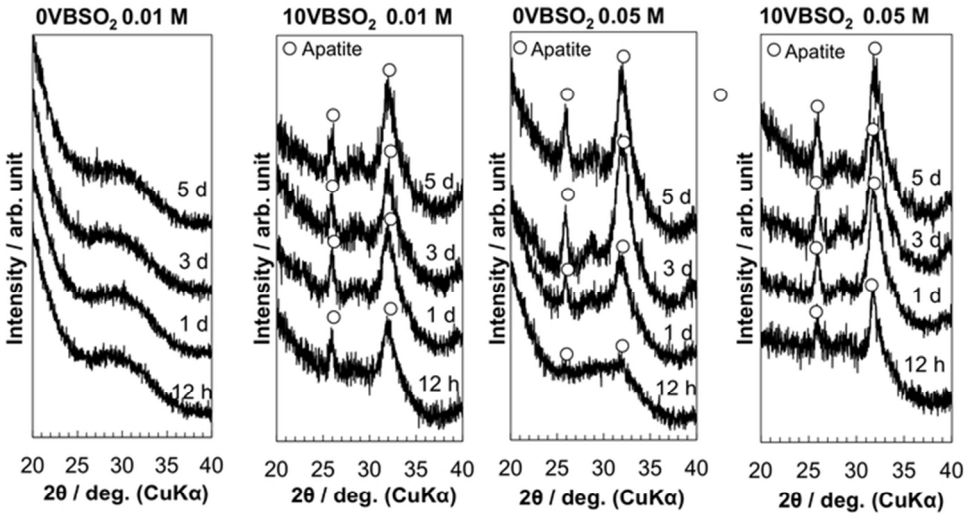

Figure 3

63x38mm (300 x 300 DPI)

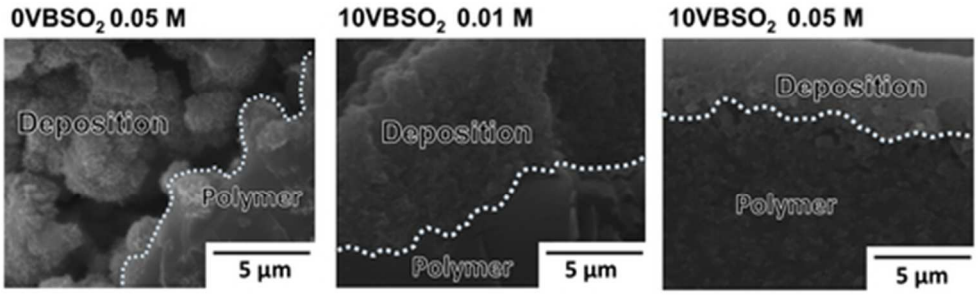

Figure 4

42x17mm (300 x 300 DPI)

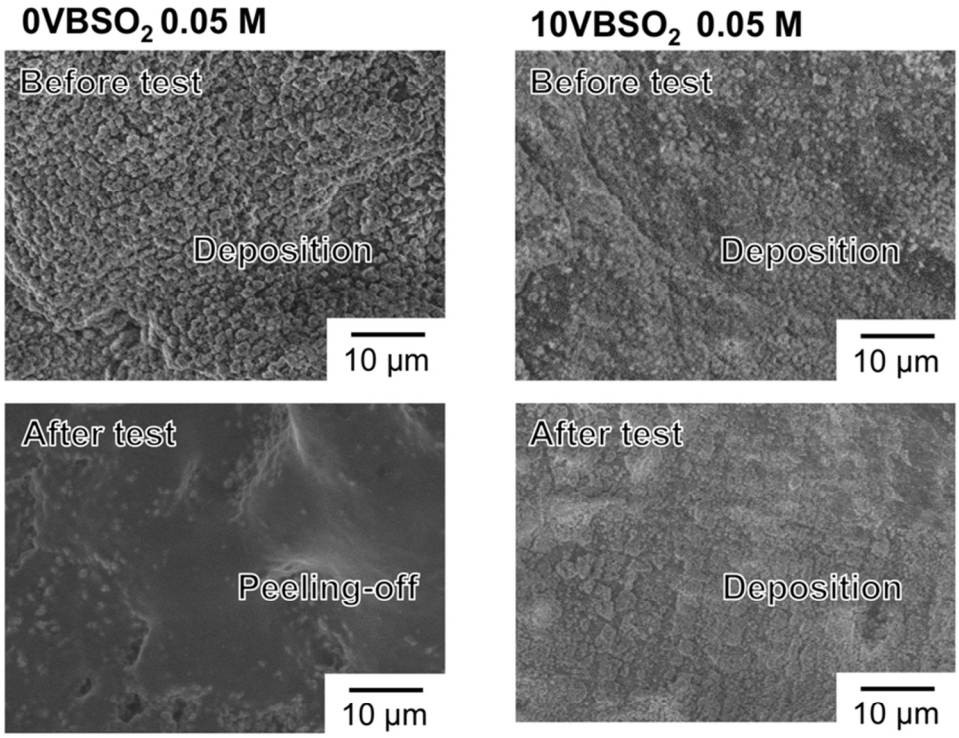

Figure 5

77x71mm (300 x 300 DPI)

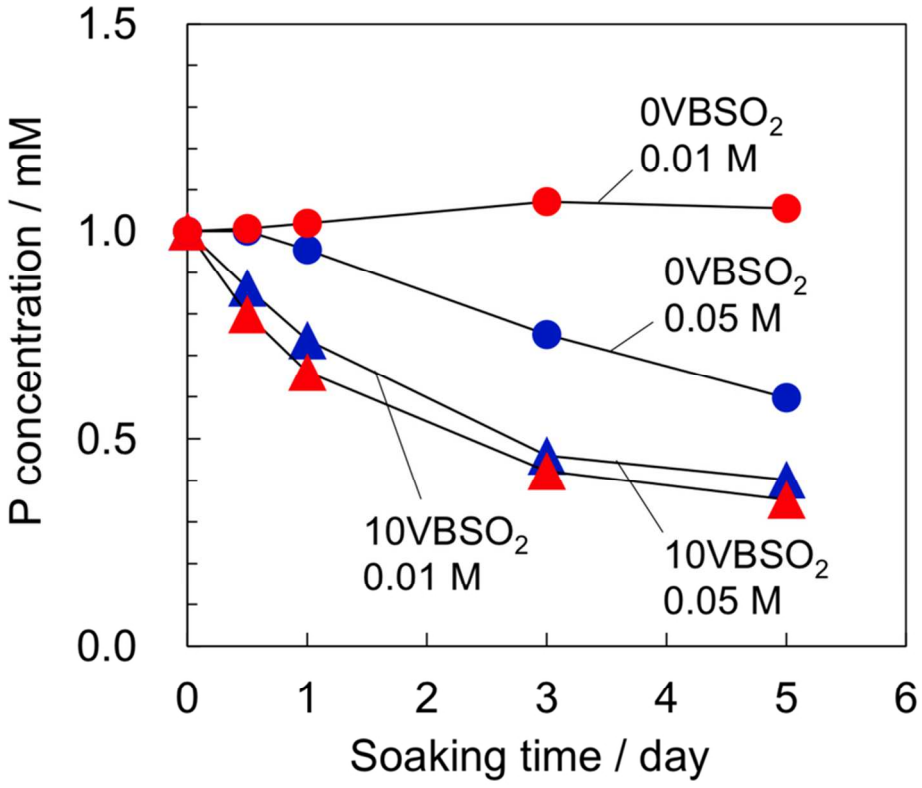

Figure 6

83x87mm (300 x 300 DPI)